Frequency Compliance of MV Voltage Sensors for Smart Grid Application

Frequency Compliance of MV Voltage Sensors for Smart Grid Application

G. Crotti, D. Gallo, *Member, IEEE*, D. Giordano, C. Landi, *Member, IEEE*,
M. Luiso, *Member, IEEE*, M. Modarres and M. Zucca

***Abstract*— With the advent of Smart Grid paradigm, Medium Voltage (MV) distribution networks have experienced great structural changes that, with the massive deployment of distributed generation, impose the network monitoring in a wider frequency range, up to some kilohertz, to evaluate power quality (PQ) phenomena and to ensure proper operation. Classical Voltage Instrument Transformers (VT) with primary rated voltages higher than a few ten of kilovolt are typically usable in a limited range around power frequency and thus for accurate measurements up to some kilohertz new types of MV sensors should be needed. Nevertheless, massive replacement of VTs in a short time is not convenient from an economic point of view. In order to delay the transition to new types of transducers, without limiting the possibility to monitor PQ, if the VTs are characterized in a wider frequency range, then their systematic deviations could be compensated with suitable digital signal processing techniques. Therefore, in this paper a calibration setup, intended to be employed both in laboratory as well as on-site, for the verification of frequency compliance of MV voltage sensors for smart grid application is presented. A comparison with the Italian National Metrology Institute (INRIM) laboratory reference system is also described.**

***Index Terms*—smart grid, medium voltage sensor, calibration, power quality, frequency response**

I. Introduction

The great structural changes that have occurred in recent years in electrical power systems with the massive deployment of distributed generation (DG) have particularly affected the Medium Voltage (MV) distribution networks causing, in many cases, significant and previously uncommon problems of power quality ([1], [2]). In this new situation, all the stakeholders are devoting much more attention in using new and more accurate monitoring systems. In particular, monitoring events occurring in frequency range up to 2.5 kHz, is an essential requirement for PQ monitoring instruments for the assessment of the compliance with standard limits ([3], [4]). A crucial point in voltage measurement at MV grids, that operate at some kilovolt, is the unavoidable utilization of step down transducers that directly affects measurement accuracy. Historically, this task has been entrusted to conventional inductive voltage transformers (VT). However, VTs with primary voltages higher than about ten kilovolt properly meet prescribed metrological requirements only in a limited range of frequencies, up to the kilohertz or lower([5], [6]).

The increased frequency range of phenomena affecting MV network requires the adoption of new high-performance transducers, which guarantee high fidelity sensing in a wider frequency range both in term of amplitude and phase ([7]-[9]). Of course, there are strong budgetary resistances that curb a massive replacement of VTs in a short time; on the other hand, the continuous monitoring of the power quality is essential in ensuring stability of the electrical grid and encourage efficiency in the energy distribution.

A partial solution to this problem can be achieved by an extension of the characterization procedure to which the conventional VTs are periodically subjected. In fact, unlike what is currently normally done, transducers can be metrologically characterized not only at the system frequency but also in a wider frequency range. These results can be used to estimate the systematic deviations and the uncertainty associated with the measurement of harmonic components; thus, if a suitable correction procedure is implemented and a correct uncertainty assessment is done, a remarkable improvement in reliability of measurement results with traditional VTs can be obtained ([10]).

A laboratory reference system for the calibration of MV VTs with distorted waveforms (from few tens of hertz up to some tens of kilohertz) has been proposed by the authors ([6]). In this paper, a further set-up for the characterization of VTs in a wide frequency range, both in laboratory and on-site, is presented. This kind of equipment can contribute to improve the knowledge of the measurement performances of traditional VT making them suitable for monitoring even high polluted distribution grid so delaying the economic effort for the installation of new transducers. In the following, the paper at first provides a brief description of the proposed calibration setup. The key element is a wideband reference voltage divider, specifically designed and realized, whose features and extended characterization are shown in the paper. The proposed set-up is validated by carrying out a VT calibration comparison with the INRIM laboratory reference system, described in [6].

II. Description of Proposed calibration System

The Fig. 1 reports a schematic representation of the proposed setup for the characterization of MV measurement voltage transformers under stationary distorted signals. Similar approaches have been used for the frequency characterization of current transformers ([11]-[13]) Dimensions, weights and characteristics of adopted devices allow the utilization of the

characterization system in laboratory, but also on-site where the transducer can be installed with a high reduction of out of service time of the device under verification. It involves an arbitrary waveform generator (Model NI 5422, ±12 V, 200 MHz, 16 bit) as a voltage signal generator that supplies a ±30 kV_{peak}, ±20 mA_{peak} portable voltage amplifier with a bandwidth of 7 kHz for large signal and 30 kHz for small signals. The characterization is performed by comparing the VT output with the measurement of the applied voltage obtained by a reference transducer parallel connected to the VT under test. Two different acquisition boards are adopted to digitize the output of VT under test (Model NI 9225, 450 V, 24 bit, 50 kHz sample rate) and of reference VD (Model NI 9239, 10 V, 24 bit, 50 kHz sample rate) respectively. Two different boards are adopted for better matching of the transducer output levels and acquisition input ranges.

A specifically designed software, developed in LabVIEW, allows an automatic management of the whole characterization procedure, limiting the required operator activity to the initial setting of test parameters, the characterization procedure starting and, after a certain time, the results collection. Basic test waveform, generated at medium voltage, is composed by the fundamental component at system frequency plus a harmonic or interharmonic component with 1 Hz resolution. In detail, it is possible to set the amplitude and the frequency of the fundamental component and the frequency, the amplitude (in percentage of the fundamental amplitude) and the initial phase angle of the other component. The software can also set a sweep of harmonic frequency and/or amplitude and/or phase angle in a specified range. The adopted generation rate is 5 MHz.

After the generation is started, the outputs of the reference and under test transducers are asynchronously and simultaneously sampled at 50 kHz. The samples acquired by the two boards, in a time interval of 1 s, are processed ([6]) in order to find frequency, amplitude and the phase of each spectral component so that it is possible to assess, for each tested frequency, the ratio and phase deviation between the VT under test and reference VD.

The presented calibration setup for the frequency characterization of VTs allows for the generation of distorted waveforms from hundreds of volt up to 22 kV_{RMS}.

This means that it is possible to characterize phase-to-ground measurement voltage transformers with a rated voltage of 30 / √3 kV up to 130% of the rated voltage. The frequency content of the distorted medium voltage signal can range from 0 Hz up to 30 kHz. The overall estimated extended uncertainty for on-site-estimation of the ratio and phase error of VTs is lower than 2 mV/V and 2 mrad respectively up to 12 kHz.

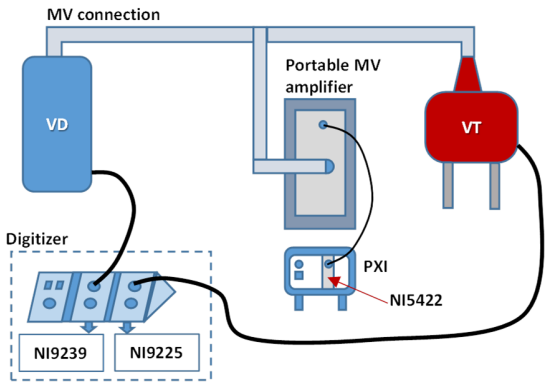

Fig. 1. Experimental Set-up for the VT frequency characterization.

It is apparent that the capabilities of the proposed characterization setup strongly depend on the metrological performances of the reference transducer so that particular attention was devoted in the design and the characterization of the reference divider, as described in the following.

III. Reference Divider Design

The main features that a reference transducer has to satisfy, in particular when stationary distorted waveforms have to be measured, are the voltage linearity and frequency flatness.

Voltage nonlinearity could provide outputs that depend on the relative phase displacement between fundamental and harmonic component. This is not acceptable for a reference transducer adopted for an accurate measurement setup aimed to estimate the ratio and phase error: in fact, in this way, the frequency behavior is dependent on the relative combination between fundamental and harmonic tones, namely their phase displacement. A flat frequency behavior of the reference transducer allows for the accurate identification of fundamental and harmonic components from the applied distorted waveforms.

The performances of the adopted VD in the frequency range from DC to 12 kHz are measured and presented in the following. In addition, as the reference transducer could be used in different environmental conditions, potential degradation of the VD metrological performances, due to proximity effect produced by metallic masses ground connected, has to be investigated. Also these aspects are carefully taken into account.

As for design specification, the rated voltage of the reference voltage divider was chosen 30 kV to allow for the calibration of most of the common MV transducers. The output of the divider is limited below 10 V_{peak} to fit to the most usual input range of the digitizers. The accuracy requirement should be restricted to two order of magnitude better than the limits fixed in [3], [4]. They prescribe that ratio error has to be better than 1 % for the 1st up to 2nd harmonics and 5 % for the 3rd up to 50th harmonics; the phase errors, instead, have to be below 1.8 mrad for the 1st up to 2nd harmonic and 90 mrad for the 3rd up to 50th harmonic. Since many applications such as distributed generations, railways, or industrial loads have disturbances up to 12 kHz, the bandwidth of the reference voltage divider is selected 12 kHz.

Four 30 MΩ resistors with rated voltage 30 kV and rated power 6 W are chosen for the MV arm of the VD. The high voltage (HV) resistors are electrically series-connected and they are physically connected in a zig-zag path. The low voltage (LV) resistor is chosen about 12 kΩ, which produces a rated Scale Factor (SF) of 10001. The structure of the resistive voltage divider (RVD) is shown in Fig. 2 (LV arm not shown).

Three metallic surfaces, gray colored, are visible. The two rounded edge plates, placed at the top and at the bottom of the structure are the high voltage and ground electrodes respectively.

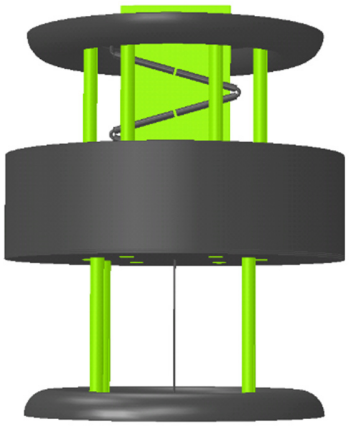

Fig. 2. FEM (finite element method) model of the reference RVD.

The cylindrical surface (with radius of 200 mm) leaning to a metallic plate, visible in the middle of the structure, is connected to the output potential of the RVD.

Such particular configuration reduces the stray capacitive coupling between the elements of the high voltage arm and ground, which cannot be easily compensated by the adjusting low voltage capacitor, which is parallel connected to the 12 kΩ LV resistor. The insulating parts (green colored in Fig. 2) mechanically support the structure of the RVD and they are chosen with a relative permittivity of 2.5. The MV resistors are connected to each other using a copper tube (4 mm thick) in order to decrease the probability of corona effect by avoiding sharp edges.

IV. Simulation of the Designed RVD

The initial design was FEM (finite element method) modelled using the numerical tool previously developed in [14]. Fig. 3 shows the simulated frequency behavior of the RVD with different shield heights. The RVD with the shield height of 120 mm provides the best results. For this shield height, the simulated electric field was reported in Fig. 4. The maximum obtained value is about 1 kV/mm. This value is low enough to consider the MV circuit sufficiently shielded in terms of electric field, making reasonably low the probability of the corona effect.

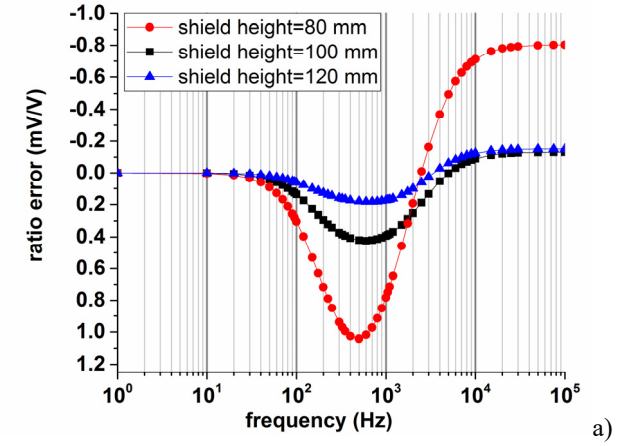

a)

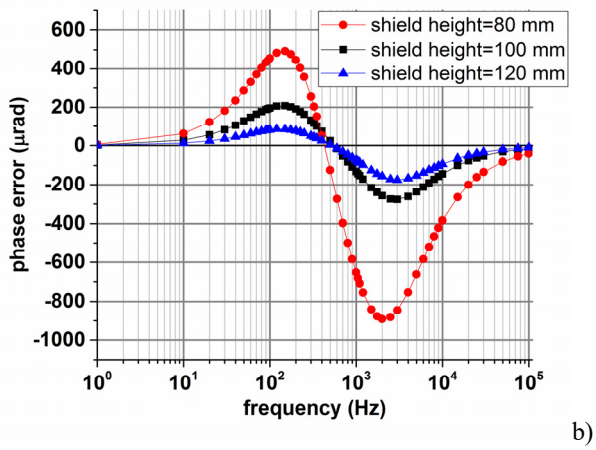

b)

Fig. 3. Frequency responses of zig-zag RVD with different shield heights

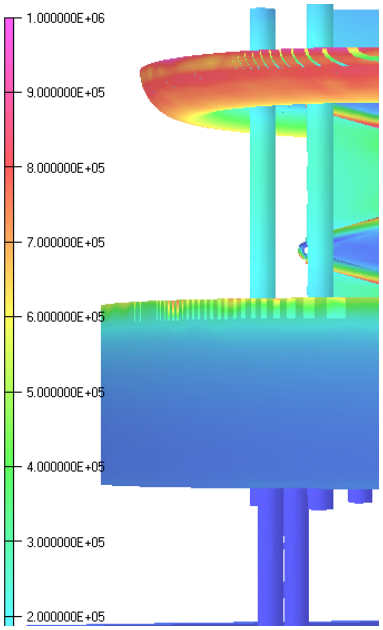

Fig. 4. Electrical field distribution in the zig-zag RVD

Although both frequency behavior and the maximum electric field are promising, there is still the proximity effect sensitivity that should be investigated. For this aim, a grounded cylindrical object with almost the same volume of the RVD was put at two different distances (500 mm and 250 mm) from the divider. The frequency behavior with and without proximity object around are shown in Fig. 5. It is clear that the RVD has a big sensitivity towards proximity changes. This happens due to the modification of the stray capacitance between the internal electrodes of the RVD and the outside objects. These kind of stray capacitances are around 1 pF or less. Therefore, adding a capacitor of much bigger value in parallel to each HV resistor can bring their effect on the frequency behavior.

Thus, a 300 pF capacitance package containing four 1.2 nF (3 kV) series-connected capacitors are added to each HV resistor. The new divider is then a resistive-capacitive VD (RCVD). The cylindrical electrode, previously connected to the output potential of the RVD is now connected to ground. The realized RVCD is shown in Fig.6 in its final version.

V. Reference Divider Low Voltage Frequency Characterization

A first characterization of the reference divider frequency flatness has been performed at low voltage (300 V) from DC to 12 kHz. The aim of this experiment is to estimate its frequency ratio (ε_r) and phase error (φ), that are defined as in ([3]):

$$\varepsilon_r(f) = k_r \cdot \frac{U_s}{U_p}(f) - 1 \qquad \varphi(f) = \varphi_s(f) - \varphi_p(f) \tag{1}$$

where k_r is the rated scale factor (the inverse of the gain of the transducer) given at the power frequency (50 Hz or 60 Hz), U_s and φ_s (U_p and φ_p) are the magnitude and phase of the transducer output voltage phasor (input voltage phasor) depending on the supply frequency. The flatness of the frequency response is defined as the maximum deviation from the mean ratio for the ratio error and the maximum phase error ($\bar{\varepsilon_r}|_{fmin \div fmax}$, $\| \varphi_{fmin \div fmax} \|_{max}$) over the considered frequency range:

$$\delta = \| \varepsilon_r(f) - \bar{\varepsilon_r}|_{fmin \div fmax} \|_{max} \qquad \rho = \|\varphi(f)\|_{max} \tag{2}$$

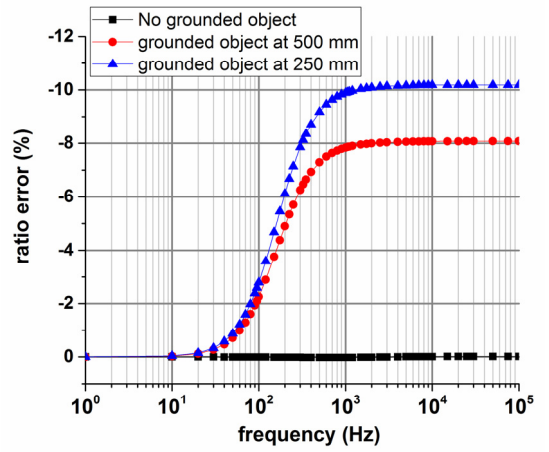

a)

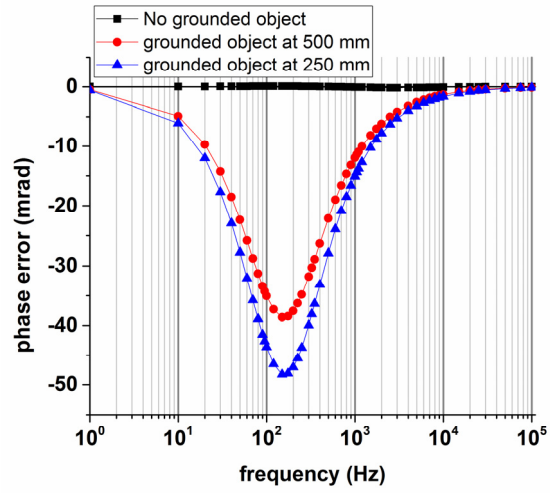

b)

Fig. 5. Ratio (a) and phase (b) frequency responses of the zig-zag RVD with a metallic object besides it

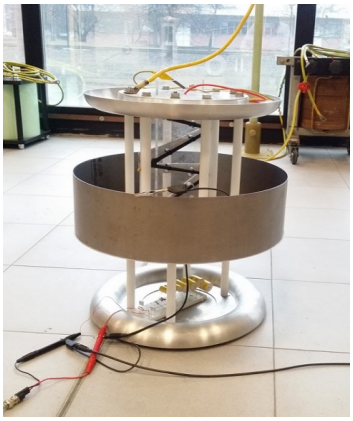

Fig. 6. The realized zig-zag RCVD

In order to test these features, the transducer has been supplied with a sinusoidal signal with fixed amplitude and variable frequency (frequency sweep) in the range of interest.

A. Description of the measurement setup

A voltage calibrator Fluke 5500A was adopted to supply the RCVD. The data acquisition system, i.e. the two synchronized boards for the acquisition of the supplied voltage and the transducer output, and the measurement software are described in [15], [16]. The accuracy of such a system (data acquisition system and measurement software) has been previously determined ([15], [16]).

The performed characterization tests provided a maximum ratio error, in the range from DC to 12 kHz, of about 100 µV/V. Higher variations were found for the phase error. At 12 kHz, the phase error reaches the value of about 20 mrad. More in details, for a fixed frequency, the analysis of 20-repeated acquisitions showed two groups of samples with two different mean values. At 10 kHz the two groups are characterized by the mean values 20 mrad and 15 mrad. A thorough analysis showed that the deviation between these two values corresponds exactly to four and three periods of the 12.8 MHz clock of the acquisition boards. Therefore, the reason of the detected phase delay was supposed to come from a trigger delay between the two-acquisition boards ranging from three to four periods of the signal clock. After the correction of the systematic part of this deviation, the phase error accuracy at 10 kHz is below 400 µrad. In addition, a second order correction was introduced to take into account the systematic mismatching between the two cut-off frequencies of the anti-aliasing filters that are embedded in the two acquisition boards. This mismatching particularly affects phase estimation. Minor impact was found on the amplitudes. The expression used in the correction of the measured phase error is:

$$\varphi_{corr}(f) = \varphi(f) - \tan^{-1}\frac{f}{f_{cut}} + \tan^{-1}\frac{f}{f_{cut+\Delta f}} \tag{3}$$

where f_{cut} is the rated cut-off frequency as defined in the board datasheet ([15]) and Δf is the mismatch between the cut-off frequencies of the two cards. Such quantity has been estimated in the digitizer characterization stage and is found to be equal to $\Delta f = 25$ Hz.

B. *Frequency analysis results*

The frequency sweep test is repeated performing a tuning of capacitance in order to obtain the best flatness in frequency response. Final results, obtained from 20 Hz up to 12 kHz, are shown in Fig. 7 demonstrating good frequency flatness. Fig. 7a provides the ratio error computed by considering a rated scale factor of 10177, which is the SF measured at DC. The ratio error ranges from -55 µV/V to 325 µV/V in the entire frequency range. For these data, δ and ρ, defined in (2), are equal to 118 µV/V and 129 µrad respectively. Such quantities reduce to 39 µV/V and 84 µrad if the considered frequency range is limited to 100 Hz – 2500 Hz that is the range defined by [3], [4].

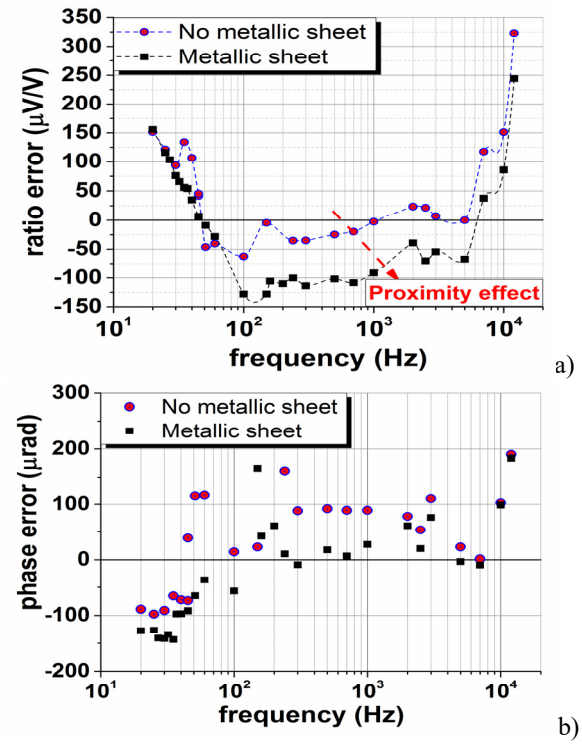

Fig. 7. Frequency behavior of the divider ratio (a) and phase (b) errors obtained by placing a metallic sheet ground connected, 30 cm far from the VD.

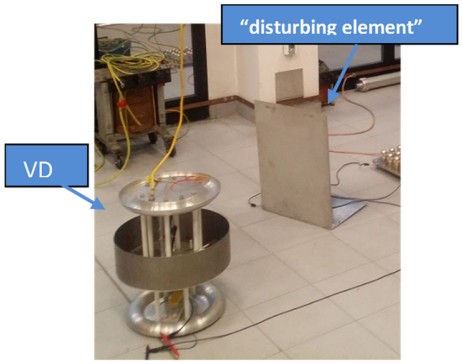

Fig. 8. Arrangement of the setup for the proximity effect investigation. On the right side, the grounded metallic sheet used as "disturbing element" can be seen.

C. *Proximity effect analysis*

The proximity effects, namely possible variations of the ratio and phase errors due to surrounding metallic masses, have to be carefully taken into account since the purpose of VD is the on-site characterization of inductive VT that are inside the substations. The adoption of a resistive-capacitive structure for the high voltage arm strongly reduces the possible variation of the equivalent high voltage capacitance produced by such metallic masses. Moreover, the proximity effect is reduced by the partial shield of the VD both at high and low voltage arm sides. Nevertheless, a set of experimental tests has been performed in order to verify the impact of proximity effect. The first test, named MS (Metallic Sheet), consists of approaching a ground connected metallic sheet to the VD (see Fig.8) and repeating the frequency analysis. The metallic sheet, with dimensions of 40 cm × 50 cm and rectangle shape, is placed 30 cm far from the VD.

In the second test, named MB (Metallic Box), the VD is placed inside a grounded metallic box with side of 80 cm. Even though the last configuration is not suitable to supply the VD at 30 kV, since the distances between the high voltage and the ground electrodes allows a maximum supply voltage of 15 kV, it stresses possible proximity effects. For this configuration, the frequency response has been repeated for two different low voltage capacitance values: the value that provided the best frequency response of the VD without grounded masses in the vicinity (C_{LV} = 771.15 nF) and the adjusted C_{LV} that improves the frequency response (C_{LV} = 770.72 nF). These last two cases are named MB1 and MB2.

Results are provided in Table I, Fig. 7 and Fig. 9. Table I summarizes the values of quantities δ and ρ with no proximity mass in the vicinity of the VD (NoP) and for the test cases MS, MB1 and MB2. Quantities δ and ρ related to NoP and MS are computed for two different frequency ranges: a narrower range, 100 ÷ 2500 Hz ([3], [4]) and a wider range, 20 ÷ 12000 Hz. The mean value of the ratio error ($\overline{\varepsilon_r}$) computed in the considered ranges is also shown.

Analyzing the effect of the metallic sheet, that is comparing MS and NoP configurations, there is a negligible impact on δ and ρ. Regarding $\overline{\varepsilon_r}$, instead, there is a shift from 46 µV/V to -99 µV/V in the 100 ÷ 2500 Hz range, which is also clearly evident in Fig. 7a.

Analyzing the effect of the metallic box, that is comparing MB1 and MB2 configurations, the quantity δ related to MB1 and MB2 is close to that measured for NoP and MS cases; instead, a considerable increase, more than one order of magnitude, is obtained for quantities ρ and $\overline{\varepsilon_r}$. As regards ρ, its high value can be explained observing Fig. 9b where an increasing behavior of phase error, with the VD inside the metallic box, is shown; moreover, the two values of C_{LV} produce the same frequency behavior. Regarding $\overline{\varepsilon_r}$, two very different values: -1036 µV/V in MB1 and 516 µV/V in MB2 configurations, are obtained. This can be explained looking at Fig. 9a: considerable shifts of the ratio error, negative for MB1 and positive for MB2, with respect to NoP configuration, can be observed.

TABLE I
VD FREQUENCY RESPONSE

	Config.	Narrow Range (100 Hz – 2.5 kHz)	Wide Range (20 Hz – 12 kHz)
$\overline{\varepsilon_r}$ / δ (μV/V)	NoP[a]	46 / 60	-2.3 / 277
	MS[b]	-99 / 60	-8 / 252
	MB1[c]	-1036 / 75	-
	MB2[d]	516 / 87	-
ρ (μrad)	NoP[a]	161	190
	MS[b]	165	184
	MB1[c]	2270	-
	MB2[d]	2220	-

[a] no proximity masses
[b] metallic sheet 30 cm from the VD
[c] metallic box with best C_{LV} (C_{LV} = 771.15 nF)
[d] metallic box with adjusted C_{LV} (C_{LV} = 770.68 nF)

As final comments on proximity effect analysis, it can be concluded that a metallic sheet has a negligible effect on VD performances.

A metallic box, which of course represents an extreme operating conditions, has a considerable effect on phase error, but does not alter the frequency flatness of the ratio error.

VI. Reference Divider High Voltage Characterization

A very important feature of a reference voltage transducer is its linearity in a wide voltage range. As a first step, the VD voltage linearity, intended as ratio and phase error maximum variations, has been measured from 2 kV up to 20 kV, at 50 Hz.

A low voltage power supply and a 100 V / 200 kV step-up transformer generate the test voltage. The VD ratio and phase errors are obtained by comparing its output with the output of a reference VT calibrated at INRIM. In particular, two reference VTs, each one with two different ratios, have been employed. The first VT, with rated ratios of 5 kV / 100 V and 10 kV / 100 V, has been used up to 12 kV. The second VT, with rated ratios of 20 kV / 100 V and 50 kV / 100 V, has been used up to 20 kV. Systematic errors associated with the reference VTs have been considered in the linearity measurement model.

The output signals are acquired by means of two synchronized Keysight 3458A multimeters and a laptop that manages the automated measuring system. Systematic errors introduced by the digitizers ([17]) are compensated. Moreover, a precise inductive VD (IVD) is connected to the output of the reference VT in order to attenuate the 100 V rated voltage output. Considering the VD rated ratio, the IVD ratio has been changed during the linearity analysis in order to provide voltages of similar amplitudes to the two digitizers. The experimental setup is shown in Fig. 10. The employed measurement software, which computes ratio and phase errors, is described in Sec. II. The extended uncertainty associated with the measured ratio and phase error is 60 μV/V and 60 μrad respectively. Measurement results are shown in Fig. 11. The maximum excursion of ratio error is about 100 μV/V, while that of phase error is about 300 μrad.

Such a good linearity of the RCVD allows to state that values of the ratio and phase errors, measured at low voltage in the DC – 12 kHz frequency range, can be considered constant when a distorted waveform, constituted by a 50 Hz high voltage fundamental component plus harmonic, is applied to the reference VD.

The overall extended uncertainties that include the RCVD

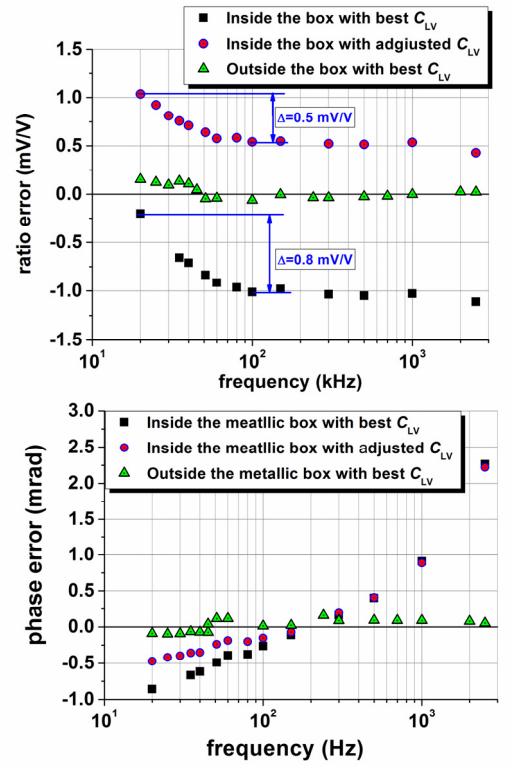

Fig. 9. Frequency behavior of the divider ratio (a) and phase (b) errors obtained by placing the divider in a grounded connected metallic box.

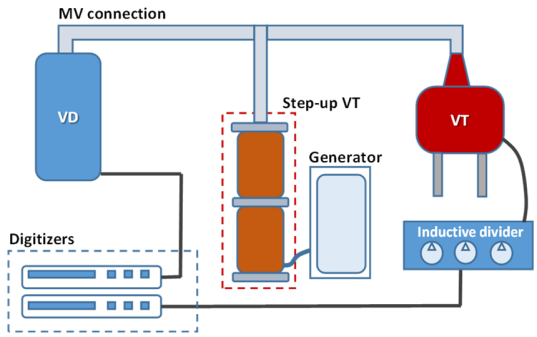

Fig. 10. Experimental Set-up for the VD linearity measurement.

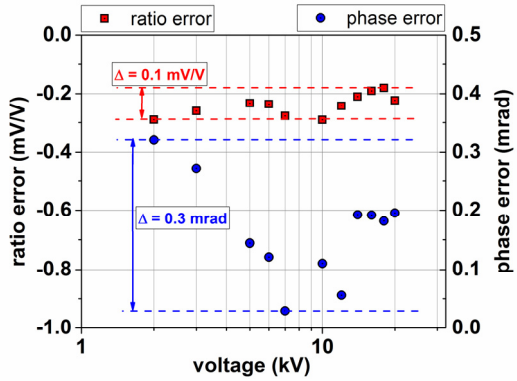

Fig. 11. VD voltage linearity in the 2 kV – 20 kV range

frequency behavior, the proximity effect, the voltage non-linearity of the divider and the acquisition system are of 500 µV/V and 500 µrad.

VII. Application To Commercial VT

The proposed calibration setup has been employed in the characterization of a commercial resin-insulated phase-to-ground inductive VT with a rated ratio of 20/√3 kV÷100/3 V. The frequency behavior has been performed by applying a fundamental signal at 60 Hz with an amplitude 20/√3 kV ad a harmonic frequency sweep from 120 Hz to 2460 Hz with a constant amplitude of 10 % of the fundamental tone. The ratio and phase error obtained by this setup have been compared with the same quantity obtained through the INRIM laboratory reference system, which exploits an absolute calibration procedure that involves two high voltage capacitors, a two-channel trans-impedance amplifier and a digitizer system.

This procedure, which is widely described in [6], requires two steps: in the first step, capacitors are parallel connected and supplied by the MV generation system, their currents are digitized and the complex ratio between them is computed. In the second step, the VT under test is parallel connected to the MV supply and one of the two capacitors is disconnected from MV supply and connected to the output of the VT. The new complex ratio of the two capacitor currents is measured; ratio error and phase displacement of the VT under test are obtained from the ratio of the complex ratios measured in the two steps.

The extended uncertainty associated with the estimate of the ratio and phase error obtained by the two-capacitance-bridge method is within 400 µV/V and 600 µrad over the considered frequency range.

Ratio and phase errors of the VT under test, measured with the two setups, are shown, respectively, in Fig. 12a and Fig. 12b.

It can be seen that the two calibration setups give always compatible results within their associated uncertainty. Deviations on SF and phase error measured with the two setups are shown in Table III.

TABLE III
DEVIATION BETWEEN SF OF VT UNDER TEST MEASURED WITH TWO DIFFERENT SETUPS

frequency. (Hz)	SF deviation (µV/V)	Phase Error deviation (µrad)
120	730	30
240	520	40
480	350	140
600	300	170
960	310	340
2460	124	720

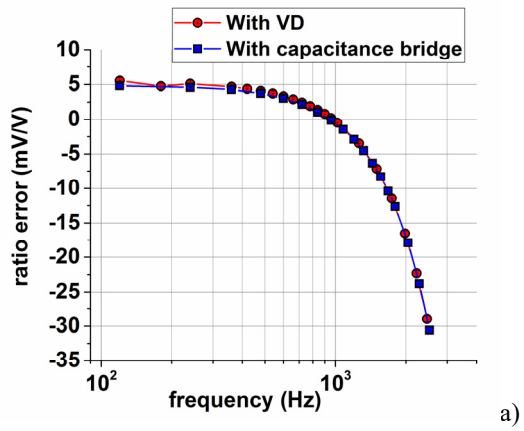

Fig. 12. Frequency behavior of the ratio (a) and phase (b) error of the commercial 20/√3 kV under test obtained by two different characterization setup: the two step capacitance bridge approach and with the developed VD as reference.

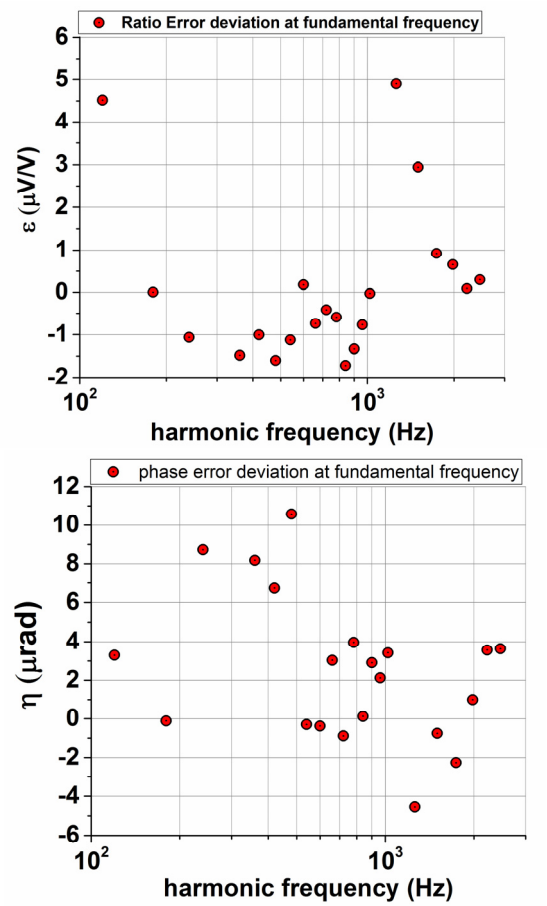

Fig. 13. Ratio (a) and phase (b) error deviations of the VT under test at the fundamental frequency extrapolated from MV distorted signals with increasing harmonic frequency. The deviation has been estimated respect to the mean value computed over the considered harmonic frequency range.

With increasing frequency, a decreasing deviation on scale factors can be appreciated, while there is an increasing deviation on phase errors. This last behavior can be explained by the frequency effect introduced by a capacitor connected to the output of the VT under test. In fact, in the characterization with the capacitance bridge, the VT output is connected to a 10 nF capacitor, while in the setup with the RCVD such capacitance value is not present. Nevertheless, the evaluated deviation can be considered acceptable being the measurement values compatible within the associated uncertainties.

The compatibility of the measurement results obtained with the proposed system, which is intended for laboratory but also for on-site, with those obtained with the INRIM laboratory reference setup then represents a validation of the measurement method.

As another proof of reliability of the proposed calibration setup, the deviations of the ratio and phase errors, measured at 60 Hz, with respect to their mean values over the entire harmonic frequency range, are shown in Fig. 13. The maximum deviation of ratio error (Fig. 13a) is 5 µV/V while the maximum deviation of phase error (Fig. 13b) is 11 µrad.

CONCLUSION

In the new context of Smart Grids, both in LV as well as MV networks, the monitoring of power quality in a wider frequency range, up to some kilohertz, is an essential task to guarantee proper network operation. Especially for MV networks, the use of voltage sensors, to scale voltage from some or tens of kilovolt down to levels compatible with measuring instruments, is unavoidable. The most installed sensors are the classical voltage instrument transformers, which can be usable in a limited frequency range. Their substitution in a short time is a not convenient task. In order to allow their use for PQ measurements, their systematic errors, introduced in magnitude and phase measurements, could be measured and accounted using proper digital signal processing techniques. Therefore, this paper has presented a calibration setup intended for frequency characterization, in non-sinusoidal conditions, of commercial VTs, both in laboratory as well as on-site. The system is composed of a portable MV amplifier, a signal generator, a digitizer and a reference Voltage Divider, specifically designed and realized. The system has been extensively characterized, leading to a first estimated uncertainty of 500 µV/V and 500 µrad for laboratory application. Moreover, the comparison with an independent measurement system confirms the metrological reliability of the proposed setup for the frequency calibration of VTs up to 12 kHz.

REFERENCES

[1] P. W. Hammond, "A new approach to enhance power quality for medium voltage AC drives," in IEEE Transactions on Industry Applications, vol. 33, no. 1, pp. 202-208, Jan/Feb 1997

[2] H. Abu-Rub, J. Holtz, J. Rodriguez and G. Baoming, "Medium-Voltage Multilevel Converters—State of the Art, Challenges, and Requirements in Industrial Applications," in IEEE Transactions on Industrial Electronics, vol. 57, no. 8, pp. 2581-2596, Aug. 2010

[3] IEC 61869-3:2011 Instrument transformers – Part 3: Additional requirements, for inductive voltage transformers, 2011.

[4] IEC/TR 61869-103 – Instrument Transformers – The use of instrument trasformers for power quality measurement, Edition 1.0 2012-05

[5] K. Kunde, H. Däumling, R. Huth, H.W. Schlierf, J. Schmid, "Frequency Response of Instrument Transformers in the kHz range", *Components & Periphery* 3 Heft 6/2012, ETZ.

[6] G. Crotti, D. Gallo, D. Giordano, C. Landi, M. Luiso and M. Modarres, "Frequency Response of MV Voltage Transformer Under Actual Waveforms," in IEEE Transactions on Instrumentation and Measurement, vol. 66, no. 6, pp. 1146-1154, June 2017

[7] G. Crotti, D. Gallo, D. Giordano, C. Landi and M. Luiso, "Medium Voltage Divider Coupled With an Analog Optical Transmission System," in IEEE Transactions on Instrumentation and Measurement, vol. 63, no. 10, pp. 2349-2357, Oct. 2014

[8] K. Kawamura, H. Saito and F. Noto, "Development of a high voltage sensor using a piezoelectric transducer and a strain gage," in IEEE Transactions on Instrumentation and Measurement, vol. 37, no. 4, pp. 564-568, Dec 1988

[9] L. H. Christensen, "Design, construction, and test of a passive optical prototype high voltage instrument transformer," in IEEE Transactions on Power Delivery, vol. 10, no. 3, pp. 1332-1337, Jul 1995

[10] I. Kollar and Y. Rolain, "Complex correction of data acquisition channels using FIR equalizer filters," in IEEE Transactions on Instrumentation and Measurement, vol. 42, no. 5, pp. 920-924, Oct 1993

[11] D. Gallo, C. Landi and M. Luiso, "Real-Time Digital Compensation of Current Transformers Over a Wide Frequency Range," in IEEE Transactions on Instrumentation and Measurement, vol. 59, no. 5, pp. 1119-1126, May 2010

[12] A. Cataliotti, D. Di Cara, A. E. Emanuel and S. Nuccio, "A Novel Approach to Current Transformer Characterization in the Presence of Harmonic Distortion," in IEEE Transactions on Instrumentation and Measurement, vol. 58, no. 5, pp. 1446-1453, May 2009

[13] A. Brandolini, M. Faifer and R. Ottoboni, "A Simple Method for the Calibration of Traditional and Electronic Measurement Current and Voltage Transformers," in IEEE Transactions on Instrumentation and Measurement, vol. 58, no. 5, pp. 1345-1353, May 2009

[14] M. Zucca, M. Modarres, D. Giordano and G. Crotti, "Accurate Numerical Modelling of MV and HV Resistive Dividers," in IEEE Transactions on Power Delivery, vol. 32, no. 3, pp. 1645-1652, June 2017

[15] G. Crotti et al., "Low cost measurement equipment for the accurate calibration of voltage and current transducers," 2014 IEEE International Instrumentation and Measurement Technology Conference (I2MTC) Proceedings, Montevideo, 2014, pp. 202-206

[16] G. Crotti; D. Gallo; D. Giordano; C. Landi; M. Luiso, "Industrial Comparator for Smart Grid Sensor Calibration," in IEEE Sensors Journal, in press, doi: 10.1109/JSEN.2017.2724299

[17] G. Crotti, D. Giordano, M. Luiso and P. Pescetto, "Improvement of Agilent 3458A Performances in Wideband Complex Transfer Function Measurement," in IEEE Transactions on Instrumentation and Measurement, vol. 66, no. 6, pp. 1108-1116, June 2017